DOI: 10.15480/882.9372

Eighth International Symposium on Marine Propulsors
smp'24, Berlin, Germany, March 2024

Noise Scaling Method and Applications for Marine Propeller with Isolated Tip Vortex Cavitation

Taegoo Lee[1, 2], Byoung-Kwon Ahn[2], Kyoungjun Lee[1] and Youngchul Lee[1]

[1]Samsung Ship Model Basin (SSMB), Ship and Offshore Performance Research Center, Samsung Heavy Industries, Daejeon, Republic of Korea

[2]Department of Naval Architecture and Ocean Engineering, Chungnam National University, Daejeon, Republic of Korea

ABSTRACT

This research reviewed the appropriate noise scaling method especially applied to merchant ships under operating conditions with an isolated tip vortex cavitation. The relation between the cavitation number and the radius of the tip vortex cavitation has been derived using the empirical vortex flow model. Two methods were presented to scale the noise source level generated by the propeller rotation. The first one is to perform the model test under the corresponding cavitation number to generate the same non-dimensional tip vortex cavity radius as that of a full-scale propeller. The scaling exponent to decide an equivalent cavitation number has been also introduced. Another is to scale the frequency and the noise source level considering the difference of the non-dimensional tip vortex cavity radius between a model and a full-scale propeller. The proposed methodology was applied to several cases of previous research and full-scale measurement data of Samsung Heavy Industries and showed acceptable results in noise level prediction. A guideline for choosing model test conditions and related scaling procedures to apply to various cases of ship operation considering the underwater radiated noise control was presented.

Keywords

Marine propeller, Tip vortex cavitation, Underwater radiated noise

1 INTRODUCTION

The underwater radiated noise from a marine propeller is the major noise source from shipping. International Maritime Organization (IMO) is preparing the guidelines to control the shipping noise properly. The essential issue is the precise prediction methodology of the noise source level at the design stage in order to meet the target level. The scaling of the measured noise source using the ship and propeller model is a practical and reliable method despite the inevitable limitations of the test environment. International Towing Tank Conference (ITTC) provides recommended procedures for noise measurement and the scaling method (ITTC 2021). Low-frequency scaling method recommended by ITTC was used for the round-robin benchmark study by Tani et al. (2020), and there were deviations among the predicted noise source levels provided by the worldwide test facilities. The scaling procedure considering the viscous effect was not applied in this benchmark test because the results of normal operating conditions with fully developed cavitation were studied. Aktas et al. (2016) presented the comparison results between the scaled noise level from the cavitation tunnel test and the full-scale measurement results for four different operating conditions for the same ship used in the round-robin test of ITTC. Aktas et al. (2016) used the noise measurement results under the same cavitation numbers as those of full-scale operating conditions when estimating the full-scale radiated noise level. The difference between the scaled noise source level and the results of full-scale measurement became larger at the condition with an isolated tip vortex cavitation. DNV (2015), LR (2018), ABS (2020), and KR (2022) specified two operating conditions in the definition of the required noise band levels. One is for a normal operating (or transit) condition, and the other is for a quiet cruise. Conventional propellers designed for commercial ships usually have fully developed cavitation under transit conditions and have considerable tip vortex cavitation, sometimes with reduced sheet cavitation, even under quiet cruise conditions. The Reynolds scale effect should be carefully considered for quiet cruise condition, where the tip vortex cavitation is the dominant noise source. The propeller cavitation under quiet cruise condition is normally an isolated tip vortex cavitation near the inception point. Therefore, the test condition considering the scale effect is necessary to simulate the tip vortex cavitation properly for this condition. Park and Seong (2017) and Park et al. (2019) introduced McCormick's exponent (McCormick 1962) into the noise scaling formulation to consider the Reynolds number effect for the tip vortex cavitation. Park and Seong (2017) used an exponent of 0.32 for the scaling of the operating condition near the cavitation inception point. The cavitation numbers of the model and full-scale propeller have been selected as each inception condition determined by the acoustic measurement along the ship speed. Lee et al. (2012) decided to use an exponent of 0.30 with model and full-scale cavitation number determined at the point of

a sudden increase in the overall sound pressure level. On the other hand, Park et al. (2019) proposed using the exponent as 0.10 based on their specific experiment results of two ship types under normal operating conditions with a fully developed cavity on the propeller blade. Several studies have concluded that the scaling exponent is also a function of the Reynolds number. Shen et al. (2009) introduced an empirical formula to determine the exponent as a function of Reynolds number. Park et al. (2021) investigated the variation in McCormick's exponent according to Reynolds number using numerical simulation. The approaches of Shen et al. (2009) and Park et al. (2021) are limited to the tip vortex cavity inception condition, in which the original McCormick exponent has been derived. Oshima (1990) explained that the scaling exponent k becomes 0.35-0.4 for a high cavitation number near the inception and becomes a smaller value for a low cavitation number. In Oshima's work, the cavity pattern was a developed tip vortex cavitation normally expected in the quiet cruise conditions for large merchant ships, and the k value for the equivalent cavitation number to make the same tip vortex cavity size was 0.15. The methodology to predict cavity size without a full-scale observation is required to determine the equivalent cavitation number for a specific operating condition. Bosschers (2020) proposed a generalized relation to scale the radius of the tip vortex cavity, which can be applied to an arbitrary operation condition.

In this study, the noise scaling method especially for the condition having an isolated tip vortex cavitation has been reviewed. The empirical vortex model (Proctor et al. 2010) gives the relation between a cavitation number and the radius of tip vortex cavitation. This relation has been used to determine the equivalent cavitation number of the model test for the specific operating condition having the same nondimensionalized tip vortex cavity size. The additional scaling can be considered when the condition of an isolated tip vortex cavitation is not able to be achieved at the equivalent cavitation number. The proposed methodology was applied to several noise source level prediction cases of previous research and the ship built by Samsung Heavy Industries.

2 NOISE MEASUREMENT AND SCALING

The noise measurement procedure of Samsung Ship Model Basin (SSMB) cavitation tunnel follows the recommended procedure of ITTC (2021) in general. The measured noise source is scaled using the relation derived in the following paragraph. This relation additionally considers the scaling effect of the tip vortex cavity size.

2.1 Test Set-up and Data Processing

The measured noise data processing of SSMB using three hydrophones follows the methodology explained below.

$$L_p = 10log_{10}\left(\frac{p^2}{p_{ref}^2}\right) \tag{1}$$

$$L'_p = 10log_{10}\left[10^{(L_{p_{s+n}}/10)} - 10^{(L_{p_n}/10)}\right] \tag{2}$$

$$L_s = L'_p - TF = L'_p - 10log_{10}\left(\frac{p_r^2}{p_i^2}\right) \tag{3}$$

$$L_s = 10log_{10}\left[\frac{1}{N}\sum_{i=1}^{N} 10^{\left(L_{s_i}/10\right)}\right] \tag{4}$$

$$L_{s,s} = L_s + \Delta SL \tag{5}$$

$$f_s = f_m\left[\frac{(r_c\ /D)_s}{(r_c\ /D)_m}\right]^{-1.0}\frac{n_s}{n_m}\left(\frac{\sigma_s}{\sigma_m}\right)^{0.5} \tag{6}$$

The measured sound pressure level, L_p in Equation (1) is transformed to a source level, L_s at a reference distance of 1m according to the procedure described by Park et al. (2020). p is a measured sound pressure of the root-mean-square value, and p_{ref} is the reference sound pressure in water (= $1\mu Pa$). The sound pressure level of the background noise, $L_{p,n}$ is measured by an additional test with the rotating dummy hub without a propeller blade under the same tunnel speed as used in the propeller noise measurement test. The background noise level, $L_{p,n}$ is subtracted from the measured sound pressure level, $L_{p,s+n}$ as the procedure of Equation (2). The transfer function, TF of the tunnel is also considered to achieve the source level, $L_{s,i}$, estimated from the position of each hydrophone. The transfer function is measured with a known source and the definition is described in Equation (3). p_r is received acoustic pressure by a hydrophone for a known source emitting p_i at the distance of $1m$. The final source level, L_s, is then calculated using the power average of the results from all hydrophones by Equation (4). The scaled source level, $L_{s,s}$, is then finally estimated by adding ΔSL which is the acoustic power increase in the full-scale operation condition as shown in Equation (5). The estimated noise spectrum can be provided along the scaled frequency given by Equation (6). r_c/D is the nondimensionalized radius of the tip vortex cavity where r_c is the tip vortex cavity radius and D is the propeller diameter. n is the propeller rotational speed, and σ is the cavitation number. The subscriptions m and s denote the model and full-scale ship respectively.

Figure 1. Test set-up for the noise measurement

2.2 Noise Scaling Relation

Park and Seong (2017) derived the collapsing time of the cavity bubble of the maximum radius based on the original work of Strasberg (1977).

$$\dot{r}(t) = \sqrt{\frac{2}{3}\frac{p_v - p_\infty}{\rho}\left\{1 - \left(\frac{r_{b,max}}{r(t)}\right)^3\right\}} \tag{7}$$

$$dt = \sqrt{\frac{3}{2}\frac{\rho}{(-\Delta p)}} \cdot \frac{r(t)^{3/2}}{\sqrt{r(t)^3 - {r_{b,max}}^3}}\, dr \tag{8}$$

$$T_c = \frac{1}{f} = 0.915\, r_{b,\,max}\sqrt{\rho\ /\ (p_\infty - p_v)} \tag{9}$$

Where r = radius of the cavity bubble; $r_{b,max}$ = maximum radius of the cavity bubble; p_∞ = reference pressure at a far field; p_v = vapor pressure; and ρ = density of a medium.

Equation (7) can be rearranged into Equation (8), and the collapsing period T_c is achieved by an integral of Equation (8) from $r_{b,max}$ to 0 as shown in Equation (9).

$$T_c \propto 0.915(r_c/D)D\sqrt{\rho\ /\ (p_\infty - p_v)} \tag{10}$$

$$\Pi_f = f(r_c/D)D\sqrt{\frac{\rho}{p_\infty - p_v}} = \frac{f(r_c/D)}{n\sqrt{\sigma}} \tag{11}$$

Equation (10) can be achieved if it is assumed that $r_{b,max}$ is proportional to the tip vortex cavity radius, r_c. The scaled frequency can be calculated according to Equation (6) derived from the dimensional analysis via Equation (11).

Levkovskii (1968) introduced acoustic power, P_a given by

$$P_a = \frac{4\pi R^2 {p'}^2}{\rho c}\Delta f = \eta_{ac} P_{pot} \tag{12}$$

Where p'^2 = mean-square sound pressure at the distance of R; and c = speed of sound at the medium having a density of ρ.

The acoustic power is expressed as the product of acoustic efficiency, η_{ac} and power due to change in potential energy, P_{pot} as expressed as in Equation (12). Baiter (1985) and Ross (1987) assumed that the acoustic efficiency is proportional to Mach number (V over c).

$$\eta_{ac} \propto \frac{V}{c} \propto \frac{\sqrt{(p_\infty - p_v)/\rho}}{c} \propto \frac{\sqrt{\sigma n^2 D^2}}{c} = \frac{nD}{c}\sqrt{\sigma} \tag{13}$$

$$\Delta P_{pot} \propto r_{b,max}^3 (p_\infty - p_v) N \propto (r_c/D)^3 \rho D^5 n^3 \sigma \tag{14}$$

ΔP_{pot} is proportional to the number of bubbles N and the volume of a collapsing bubble per a second in the group of bubbles having the maximum radius of bubble, $r_{b,max}$ as shown in Equation (14).

$$\Pi_p \propto \frac{P_a}{\eta_{ac} P_{pot}} \propto \frac{1}{\eta_{ac}} \frac{R^2 {p'}^2}{\rho^2 c (r_c/D)^3 D^5 n^3 \sigma}\Delta f \tag{15}$$

$$\Pi_p \propto \frac{c}{nD\sqrt{\sigma}} \frac{R^2 {p'}^2}{\rho^2 c (r_c/D)^3 D^5 n^3 \sigma} \frac{n\sqrt{\sigma}}{(r_c/D)} = \frac{R^2 {p'}^2}{\rho^2 (r_c/D)^4 D^6 n^3 \sigma} \tag{16}$$

$$\frac{{p'_{s,1Hz}}^2(f_s)}{{p'_{m,1Hz}}^2(f_m)} = \left(\frac{n_s}{n_m}\right)^3 \left[\frac{(r_c\ /D)_s}{(r_c\ /D)_m}\right]^4 \left(\frac{D_s}{D_m}\right)^6 \left(\frac{\sigma_s}{\sigma_m}\right) \times \left(\frac{\rho_s}{\rho_m}\right)^2 \left(\frac{R_m}{R_s}\right)^2 \tag{17}$$

$$\Delta SL = 20log_{10}\left\{\left(\frac{R_m}{R_s}\right)^{1.0}\left(\frac{n_s D_s}{n_m D_m}\right)^{1.5}\left(\frac{D_s}{D_m}\right)^{1.5}\right\} + 20log_{10}\left\{\left(\frac{\sigma_s}{\sigma_m}\right)^{0.5}\left[\frac{(r_c\ /D)_s}{(r_c\ /D)_m}\right]^{2.0}\right\} \tag{18}$$

Equation (17) is derived from the dimensional analysis as Equation (15) and (16) using the relation of Equation (13) and (14). The increase of scaled source level is expressed as Equation (18) following the convention of ITTC (2021).

3 SCALING METHOD OF TIP VORTEX CAVITY SIZE

The ratio of the nondimensionalized vortex cavity radius between the model and the full-scale propeller at each cavitation number can be determined using the empirical vortex model proposed by Proctor (2010). This relation is used in the noise scaling procedure expressed as Equation (6) and (18). An example of the noise scaling procedure for the operating condition having the isolated tip vortex cavitation is introduced.

3.1 Empirical Relation of Tip Vortex Cavity Radius

The relationship between the cavitation number and cavity size can be derived from the vortex model describing the tangential velocity distribution. Hommes et al. (2015) compared the tangential velocity and pressure distribution from various vortex models with the experimental data. The empirical vortex model considering the effect of roll-up proposed by Proctor et al. (2010) is such a model that provides values close to the experimental results.

$$\bar{v}_\theta(\bar{r}) = \frac{1}{\bar{r}}\left[1 - exp\left\{-\zeta_1\left(\frac{\bar{r}}{B/r_v}\right)^{0.75}\right\}\right],\ \bar{r} > 1.4 \tag{19}$$

$$\bar{v}_\theta(\bar{r}) = 1.0939\frac{1}{\bar{r}}\left[1 - exp\left\{-\zeta_1\left(\frac{1.4}{B/r_v}\right)^{0.75}\right\}\right] \times [1 - exp\{-\zeta(\bar{r})^2\}], \bar{r} \le 1.4 \quad (20)$$

Where $\bar{r} = r/r_v$, non-dimensionalized radius of vortex; r_v = radius of vortex core (viscous core); $\bar{v}_\theta = v_\theta/(\Gamma_\infty/2\pi r_v)$, non-dimensionalized tangential velocity; v_θ = tangential velocity; and Γ_∞ = initial circulation of vortex.

The formulation of the tangential velocity in a vortex cross-section of Proctor's model is presented as Equations (19) and (20). The length of wing span (radius of propeller), B, is introduced to consider the vorticity roll-up region. The Proctor's vortex model also has the flexibility to adapt to a specific vortex core size using tuning factors. The tuning factors are ζ = 1.2527 and ζ_1 = 10 as recommended by Proctor et al. (2010). The tangential velocity distributions of various vortex models are compared with that of Proctor's vortex model in Figure 2.

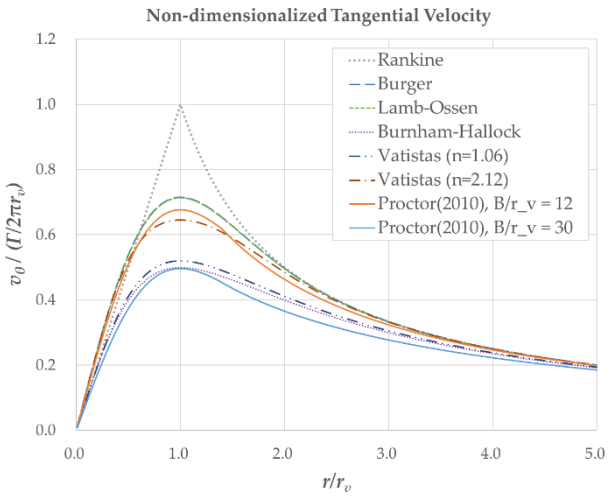

Figure 2. Tangential velocities along the vortex radius by various empirical models

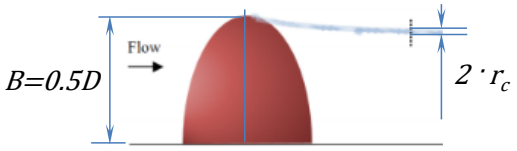

Figure 3. Conceptual diagram of the tip vortex cavitation

The non-dimensional form of the cavitation number, σ/σ_i, can be expressed using the tangential velocity of vortex flow in the integral form. It is assumed that p_v equals p_{min} at the condition of the cavity inception.

$$\int_{p(r)}^{p(\infty)} dp = p_\infty - p_r = \int_r^\infty \rho\frac{{v_\theta}^2}{r^*}dr^* \quad (21)$$

$$\frac{\sigma}{\sigma_i} = \frac{p_\infty - p_v}{p_\infty - p_{min}} = \frac{\int_{r_c}^\infty \rho\frac{{v_\theta}^2}{r^*}dr^*}{\int_0^\infty \rho\frac{{v_\theta}^2}{r^*}dr^*} \quad (22)$$

Where p_∞ = pressure at $r \to \infty$; p_v = vapor pressure at $r \to r_c$; r_c = radius of vortex cavitation; and p_{min} = minimum pressure at $r \to 0$.

The numerical integration of Equation (22) gives the relation between the cavitation number and tip vortex cavity size. The inverse function of Equation (22) gives a nondimensionalized tip vortex cavity radius, r_c/r_v according to the cavitation number.

$$\frac{r_c}{r_v} = f\left(\frac{\sigma}{\sigma_i}\right) \quad (23)$$

B/r_v used in Equation (22) and (23) can be achieved from an iterative process using the relation with the target cavitation number and the measured value of B/r_c.

$$\frac{B}{r_v} = \frac{B}{r_c}\cdot\frac{r_c}{r_v} = \frac{B}{r_c}\cdot f(\sigma/\sigma_i\ ,\ B/r_v) \quad (24)$$

B/r_v of a full-scale propeller can be evaluated with a ratio of cavitation numbers at inception between the model and full-scale as provided by Bosschers (2018). The ratio of cavitation numbers at inception can be determined with a separate cavitation inception test with a model propeller and the scaling relation proposed by McCormick (1962).

$$(B/r_v)_s = \left(\frac{\sigma_{i,s}}{\sigma_{i,m}}\right)^{0.5}(B/r_v)_m \quad (25)$$

$$\frac{\sigma_{i,s}}{\sigma_{i,m}} = \left(\frac{Re_s}{Re_m}\right)^{k_i} \quad (26)$$

Where Re = Raynolds Number; and k_i = scaling exponent.

Now, the ratio of the non-dimensionalized radius of the tip vortex cavity can be derived from Equation (23) and (25).

$$\frac{(r_c\ /D)_s}{(r_c\ /D)_m} = \frac{(r_c\ /\ r_v)_s}{(r_c\ /\ r_v)_m}\frac{(r_v\ /D)_s}{(r_v\ /D)_m} \quad (27)$$

$$\frac{(r_c\ /D)_m}{(r_c\ /D)_s} = \left(\frac{\sigma_{i,s}}{\sigma_{i,m}}\right)^{0.5}\frac{f_{(B/r_v)_m}[(\sigma\ /\ \sigma_i)_m]}{f_{(B/r_v)_s}[(\sigma\ /\ \sigma_i)_s]} \quad (28)$$

Measured r_c in model test condition and the inception cavitation number give a ratio of the nondimensional tip vortex cavity radius at the target ship operation condition, σ_s, through the Equation (28) using Proctor's empirical vortex model.

3.2 Procedure of the Tip Vortex Cavity Scaling

The proposed vortex scaling method has been applied to the target ship designed and built by Samsung Heavy Industries as shown in Figure 4. The details of the propeller are described in Table 1. The interested ship speed is 11.1kts as the quiet cruise condition, and the full-scale noise measurement has been performed at this ship speed. The corresponding cavitation number at 11.1kts is lower than the inception cavitation number of the model scale, $\sigma_{i,m}$. There is an isolated tip vortex cavitation having a smaller radius than that of the full-scale propeller at this condition as shown in Figure 5. The nondimensionalized radius of the model scale tip vortex cavity is 0.600 at the nondimensionalized model cavitation number 0.761. The viscous core radius of a tip vortex at the model scale has been determined in the iterative calculation with Equation (24). The blue line in Figure 6 is the relation for the model scale propeller tip vortex cavitation. The black dashed line is the relation for the full-scale tip vortex cavitation using the viscous core radius from Equation (25).

Figure 4. Target vessel of noise scaling: Aframax crude oil tanker, AURVIKEN (source: MarineTraffic.com)

Table 1. Principal dimension of model propeller

Diameter	245.0mm
Number of Blades	4
Pitch Ratio(P/D) at 0.7R	0.812
Chord-length Ratio(C/D) at 0.7R	0.256

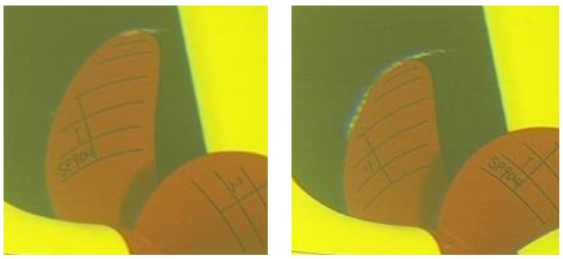

Figure 5. Cavitation observation on the model propeller of the target vessel at quiet cruise condition (V_s = 11.1kts)

The cavitation number for the full-scale tip vortex cavity inception has been determined by Equation (26). The exponent of Reynolds number scaling is 0.3 based on the research with a similar ship type by Lee et al. (2012).

Figure 7 shows the curve of the nondimensionalized tip vortex cavity radius ratio according to the model cavitation number for the condition corresponding to the ship speed of 11.1kts. Each ship operating condition has one curve of this relation, and the ratio of the tip vortex size can be determined at each model cavitation number.

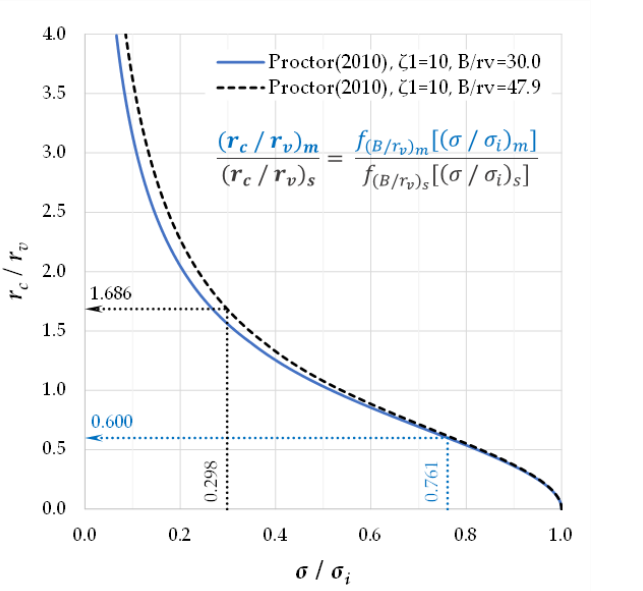

Figure 6. The radius of the vortex cavitation according to each cavitation number at the model and full-scale condition corresponding to 11.1kts of the target vessel

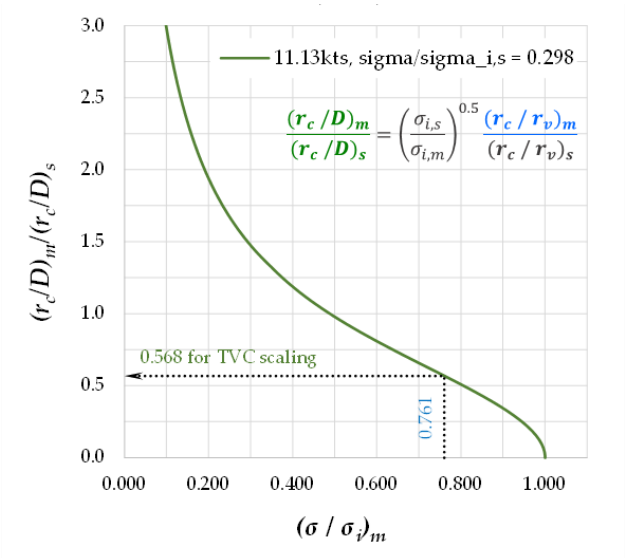

Figure 7. The ratio of the nondimensionalized tip vortex cavity radius according to the cavitation number at the model test for the scaling of the condition at 11.1kts of ship speed

The model test condition having an isolated tip vortex cavitation is usually limited to a certain range. The inception point of the sheet cavitation usually starting from the leading edge of the propeller blade is not far from that of the tip vortex cavity inception. Any cavitation number between these two inception points can be chosen as the test condition for the tip vortex cavity scaling. The model test condition corresponding to $(\sigma/\sigma_i)_s$ = 0.761 is slightly higher than the cavitation number of the sheet cavity inception, therefore this is the lowest cavitation number for the isolated tip vortex cavitation in this test. The ratio of the nondimensionalized tip vortex cavity radius is 0.568, and this means the relative size of the tip vortex radius is 56.8% of the full-scale tip vortex cavity radius. The measured noise source level can be additionally scaled using this ratio according to Equation (6) and (18).

3.3 Scaling Exponent for the Equivalent Tip Vortex Cavity Radius

The model cavitation number for the equivalent radius of the tip vortex cavitation can be calculated at the point giving $(r_c/D)_m/(r_c/D)_s = 1$. Two ship speed conditions of the target vessel are introduced to show the difference in the application of the tip vortex cavity scaling method. 7.3kts and 11.1kts are these two speed conditions, and Point A to Point D are described in Table 2 and Table 3 respectively. The definition of each test condition is explained below.

Point A: Test condition with the same cavitation number as the target ship speed.

Point B: The inception point of the tip vortex cavity in the model test. This is the interpolated point on the operating curve from several inception points with the test varying thrust coefficient.

Point C: The test condition with an equivalent cavitation number for the tip vortex cavity scaling. The value of $(r_c/D)_m/(r_c/D)_s$ is 1 at this point.

Point D: The selected model test condition used in the noise prediction for the target ship speed. Point C is the best choice if it is a higher cavitation number than the sheet cavitation inception point. Alternative condition could be chosen as near as possible to Point C before the tip vortex cavity is mixed with the sheet cavitation.

Table 2. Model test conditions and corresponding radius of tip vortex cavitation for 7.3kts of ship speed

Condition	A	B	C, D
Corresponding Ship Speed, Vs	7.3kts	9.7kts	10.7kts
$(r_c/D)_m/(r_c/D)_s$	-	-	1.000
Corresponding Cavitation No, σ	12.999	7.397	6.129

Table 3. Model test conditions and corresponding radius of tip vortex cavitation for 11.1kts of ship speed

Condition	B	A, D	C
Corresponding Ship Speed, Vs	9.7kts	11.1kts	13.7kts
$(r_c/D)_m/(r_c/D)_s$	-	0.568	1.000
Corresponding Cavitation No, σ	7.397	5.626	3.615

As shown in Table 2, the test condition corresponding to an equivalent tip vortex cavity radius (=Point C) is in between the inception condition for the tip vortex and the leading edge sheet cavitation. The additional tip vortex cavity scaling is not necessary when the noise is measured at this condition. The corresponding cavitation number is 6.129 and $(\sigma/\sigma_i)_m$ is 0.829 as shown in Figure 8. As already explained in the previous paragraph, Point C for 11.1kts is at a lower cavitation number than the inception condition of the leading edge sheet cavitation. Therefore, Point A is the best option for the test condition for the full-scale estimation. In spite of the limitation of the test cavitation number, the ideal cavitation number for the equivalent tip vortex cavity radius has been calculated in both ship speed conditions in Figure 8. The exponents of Reynolds number scaling expressed as k_{ce} can reversely be calculated using the equivalent cavitation number.

$$\frac{\sigma_s}{\sigma_m} = \frac{(\sigma_s/\sigma_{i,s})}{(\sigma_m/\sigma_{i,m})}\frac{\sigma_{i,s}}{\sigma_{i,m}} = \left(\frac{Re_s}{Re_m}\right)^{k_{ce}} \tag{29}$$

$$k_{ce} = \frac{\log_{10}\left(\frac{\sigma_s/\sigma_{i,s}}{\sigma_m/\sigma_{i,m}}\right) + k_i \log_{10}\left(\frac{Re_{i,s}}{Re_{i,m}}\right)}{\log_{10}\left(\frac{Re_s}{Re_m}\right)} \tag{30}$$

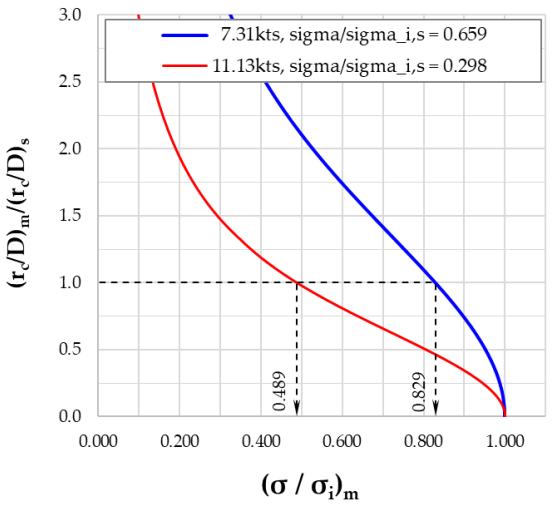

Figure 8. Cavitation number of the model tests equivalent to the same nondimensionalized radius of the tip vortex cavity

The exponent k_{ce} at the condition having a developed tip vortex cavitation is different from k_i at the inception condition introduced by McCormick (1962). Figure 9 shows the calculated exponent k_{ce} according to the full-scale cavitation number corresponding to the ship operation condition using Equation (30). There are different curves for each Reynolds number in Figure 9. The flow speed of the cavitation tunnel at the inception test and 7.3kts condition is different from that of the 11.1kts condition. The model propeller rotational speed at the test for 11.1kts is lower than the others, therefore there is a higher deviation from the other results. The exponent k_{ce} gradually decreases as the cavity becomes stronger. k_{ce} starts from 0.3 which is identical to the exponent at inception, k_i, and becomes 0.229 at 7.3kts condition and 0.127 at 11.1kts condition. The smaller scaling exponent is applied to find an equivalent cavitation number for the condition with a stronger tip vortex cavity.

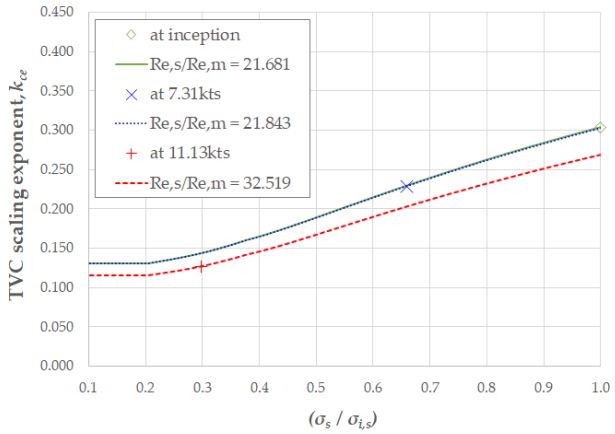

Figure 9. Scaling exponent for the tip vortex cavitation size according to the full-scale ship operation condition

3.4 Sensitivity Study on the Empirical Vortex Model

The empirical vortex model proposed by Proctor (2010) has tuning factors. The viscous core size expressed as B/r_v and the scaling exponent at inception also can make a change in the final result. The sensitivity of each component to the final result of noise scaling has been studied with the example of scaling for 11.1kts presented in the previous paragraph. The tuning factor ζ_1, B/r_v, and k_i are varied within arbitrary ranges and the resultant errors in the increase of source level were calculated. Table 4 is the result of varying the tuning factor ζ_1 from 5 to 20. The relations between the cavitation number and the tip vortex cavity size both in the model and the full-scale are changed, and the resultant relations of the ratio of the non-dimensionalized tip vortex cavity radius are also adjusted and give different values at the target cavitation number as shown in Figure 10.

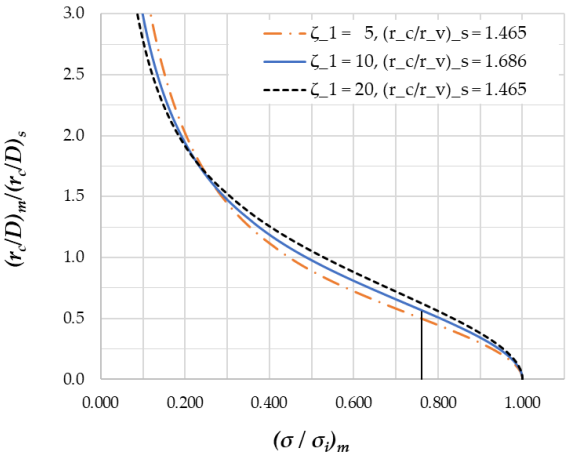

Figure 10. Sensitivity analysis of the ratio of nondimensionalized tip vortex cavitation radius for Proctor's vortex model with coefficient ζ_1

Half and two times of ζ_1 make errors of 2.2dB and -1.7dB respectively. Keeping the default value of ζ_1 as 10 proposed by Proctor (2010) is acceptable considering this level of sensitivity.

Table 4. Sensitivity analysis for Proctor's vortex model with coefficient ζ_1

ζ_1	k_c	$(r_c/D)_m/(r_c/D)_s$	$\Delta SL_{error}[dB]$
5	0.000	0.500	2.2
10	0.000	0.568	-
20	0.000	0.625	-1.7

B/r_c is obtained from the measurement during the cavitation observation. Image processing from the cavity photos can give the average size of r_c. The tip vortex cavitation boundary can be ambiguous due to the shape of the developed cavity and the resolution of the image files. Due to this reason, the effect of the error in B/r_c on the level of the noise scaling has been investigated to check the acceptable allowance. The positive and negative deviations of 10 for the measurement of B/r_c makes the differences of -0.5dB and 0.4dB respectively in the final scaled source levels as shown in Table 5.

Table 5. Sensitivity analysis for Proctor's vortex model with coefficient B/r_c

B/r_c	k_c	$(r_c/D)_m/(r_c/D)_s$	$\Delta SL_{error}[dB]$
40	0.000	0.584	-0.5
50	0.000	0.568	-
60	0.000	0.556	0.4

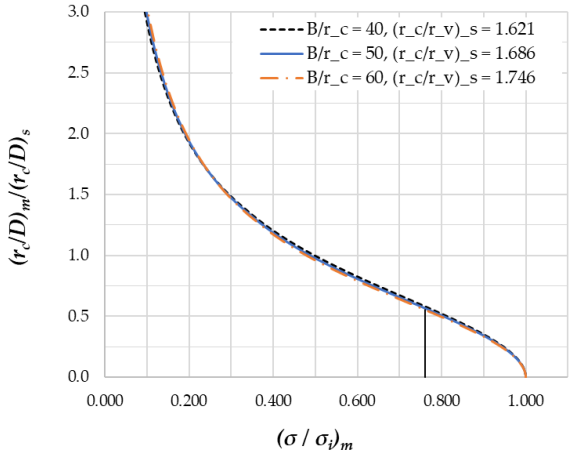

Figure 11. Sensitivity analysis of the ratio of nondimensionalized tip vortex cavitation radius for Proctor's vortex model with coefficient B/r_c

The scaling exponent at the tip vortex cavitation inception, k_i, is not a component of Proctor's empirical vortex model. However, the ratio between the cavitation inception number of the model and full-scale is the major term for the evaluation of the scaled tip vortex cavity radius as in the Equation (28). k_i of 0.3 has been used in the example of the previous paragraph, and the result from an additional scaling work with k_i of 0.4 has been studied to see the amount of error on the final scaled source level. The r_c/r_v according to the cavitation number at the model scale with k_i of 0.4 is the same as that with k_i of 0.3, but the relations at full-scale become different due to the change of $(B/r_v)_s$ according to the Equation (25). The amount of error for this case is 1.6dB based on the difference of the tip vortex cavity radius ratio as shown in Table 6.

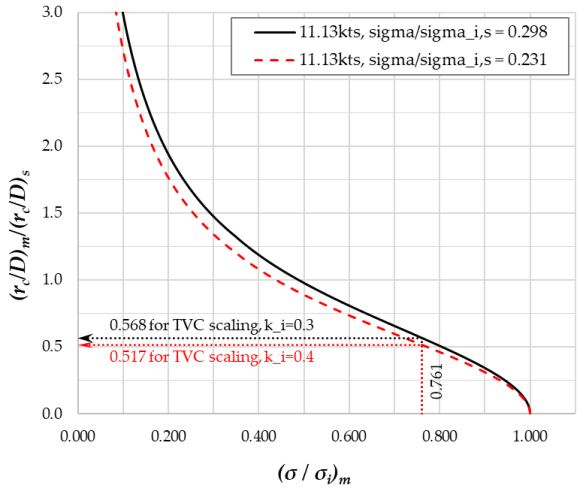

Figure 12. Sensitivity analysis of the ratio of nondimensionalized tip vortex cavitation radius for Proctor's vortex model with scaling exponent for the cavity inception, k_i

Table 6. Sensitivity analysis for Proctor's vortex model with scaling exponent for the cavity inception, k_i

k_i	k_c	$(r_c/D)_m/(r_c/D)_s$	$\Delta SL_{error}[dB]$
0.3	0.000	0.568	-
0.4	0.000	0.517	1.6

4 APPLICATIONS AND DISCUSSIONS

The present method of the tip vortex cavity scaling has been applied in the examples from the previous works of literature and the target vessel of this paper. Several assumptions on the unknown components within the range of the deviation studied in the previous chapter could be acceptable because the effect on the final scaled source level is not significant.

The first case is the reproduction of the works by Oshima (1990). There is a full-scale measurement corresponding to the cavitation number of 3.56 with the propeller rotational speed of 140rpm. An isolated tip vortex cavity on the face side of the blade near the tip is observed as shown in Figure 13.

Figure 14 shows the ratio of the nondimensionalized tip vortex cavity radius according to the model cavitation number calculated with the exponent k_i at inception used in the literature as 0.35. The equivalent cavitation number for the same relative tip vortex cavity radius as the full-scale one is calculated as $(\sigma/\sigma_i)_m = 0.715$.

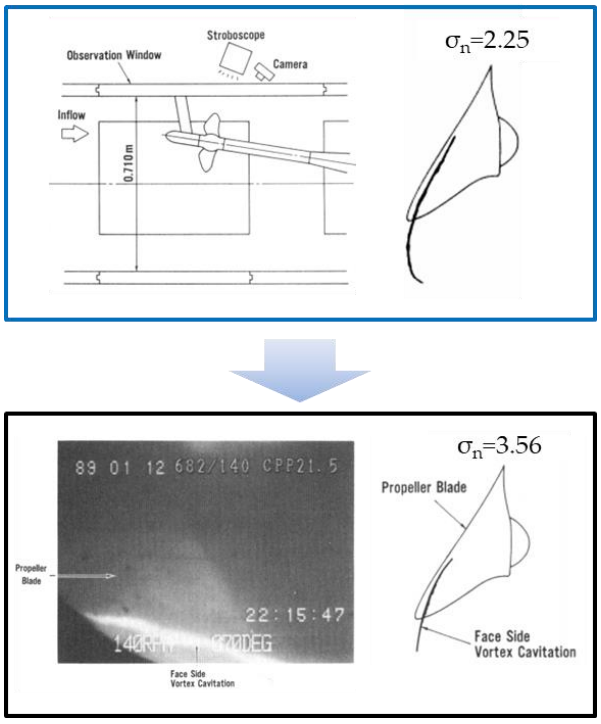

Figure 13. Comparison of the tip vortex cavitations between the model test and the full-scale observation of the ship having twin CPP, Oshima(1990)

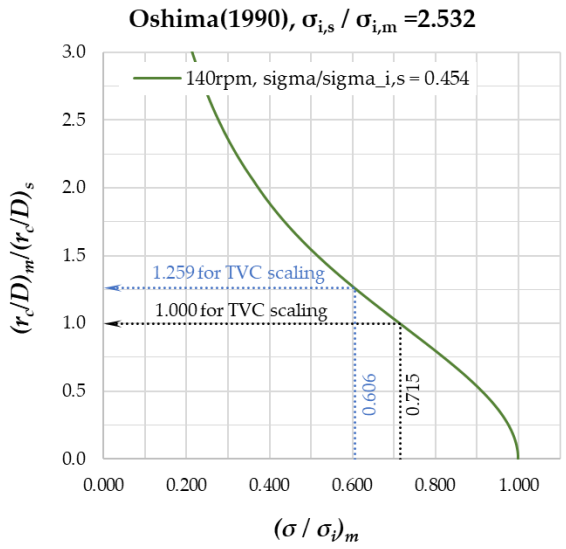

Figure 14. The ratio of the nondimensionalized tip vortex cavity radius according to the model cavitation number for σ_s =3.56

The nearest test condition to this equivalent cavitation number is $(\sigma/\sigma_i)_m$ = 0.606, and the sketch of the cavity at this condition with σ_m = 2.25 is shown in Figure 13. The radius of the tip vortex cavity generated in the model test is larger than the full-scale one. $(r_c/D)_m/(r_c/D)_s$ is 1.259 in this case, and this means that the nondimensionalized radius of the tip vortex at this model test condition is 1.259 times higher than that of the full-scale operation with 140rpm. The final scaled noise source level is reduced with this relation using Equation (18). This procedure can be used when the test at an equivalent tip vortex cavity radius is not available as in this example.

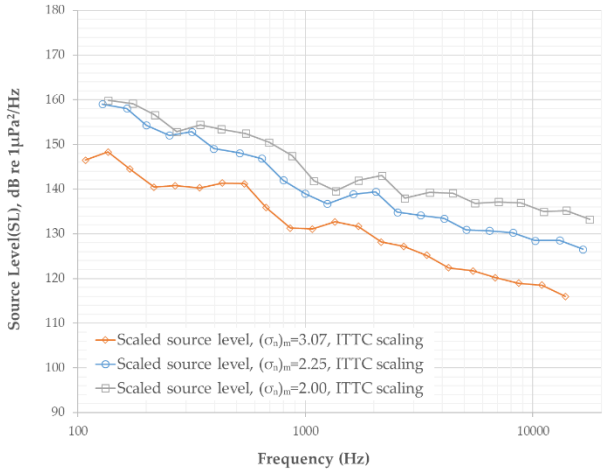

Figure 15. Scaled source level according to the recommended procedure of ITTC for the full-scale condition of σ_s =3.56, Reproduction of work by Oshima (1990)

There are two more test conditions higher and lower than σ_n = 2.25. These two noise measurement results can also be used to estimate the full-scale source level with an additional tip vortex cavity scaling. The scaled source level with each noise measurement result using the recommended procedure of ITTC (2021) in Figure 15 is adjusted with the additional tip vortex cavity size scaling and converged into a similar level for the target condition of $(\sigma_n)_s$ = 3.56 as shown in Figure 16. The scaled source levels with the test results at $(\sigma_n)_m$ = 2.25 and $(\sigma_n)_m$ = 3.07 are compared with the full-scale measurements in Figure 17 and Figure 18. The scaled source level with the present method including the tip vortex cavity scaling shows better agreement along the entire frequency band.

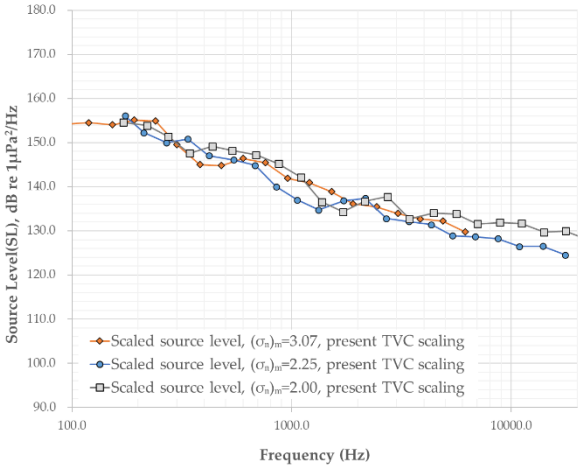

Figure 16. Scaled source level according to the present method using tip vortex cavity scaling for the full-scale condition of σ_s =3.56

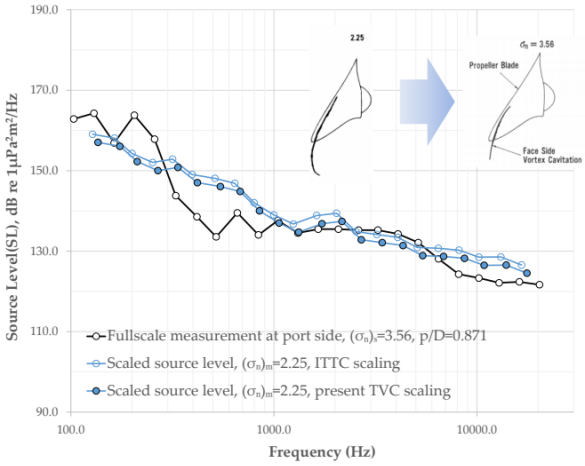

Figure 17. Comparison between the full-scale measurement result and the scaled level using the model test result at $\sigma_{n,m}$ = 2.25 by Oshima(1990)

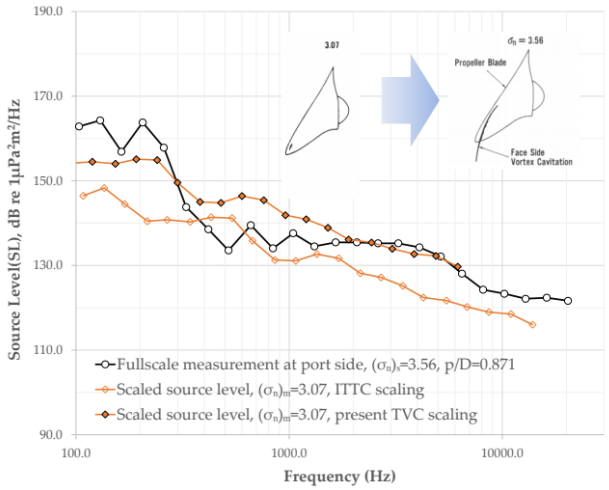

Figure 18. Comparison between the full-scale measurement result and the scaled level using the model test result at $\sigma_{n,m}$ = 3.07 by Oshima(1990)

The second validation case for the application of the present scaling method is the comparison result by Lee et al. (2021). The full-scale noise measurement with the flush-mounted hydrophones on the hull surface was conducted with a crude oil tanker at various ship speeds. The inception condition of the suction side tip vortex cavitation is summarized in Table 7. $\sigma_{i,s}/\sigma_{i,m}$ is 2.767 and the corresponding scaling exponent k_i is 0.3. Two different approaches are studied to show the applicability of the present tip vortex scaling method. Two model test cases corresponding to the cavitation numbers for 16.0kts and 17.0kts of the ship speed are used in the first study.

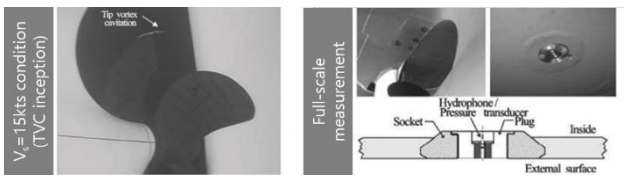

Figure 19. Noise measurement and cavity observation in the cavitation tunnel and full-scale noise measurement by Lee et al. (2012)

Table 7. Summary of the cavitation inception condition by Lee et al. (2012)

	Model ship	Full ship
Ship speed	15.0kts	8.8kts
Cavitation number, σ_n	3.833	10.604
Reynolds number, R_e	0.91×10^6	2.53×10^7

The target ship speed of the noise scaling is 14.6kts. The isolated tip vortex cavitation is expected at this ship speed based on the model and full-scale inception speed. $(\sigma/\sigma_i)_s$ is 0.382 for 14.6kts operation condition, and $(r_c/D)_m/(r_c/D)_s$ according to the model test cavitation number in this ship speed is presented in Figure 20. The scaling ratios of the tip vortex radius are 0.506 at $(\sigma/\sigma_i)_m$ = 0.880 for the test condition of 16.0kts, and 0.751 at $(\sigma/\sigma_i)_m$ = 0.754 for the test condition of 17.0kts respectively. The larger increase of noise source level is necessary with the noise measurement result at a cavitation number of 16.0kts where the tip vortex radius was smaller than that for the 17.0kts condition.

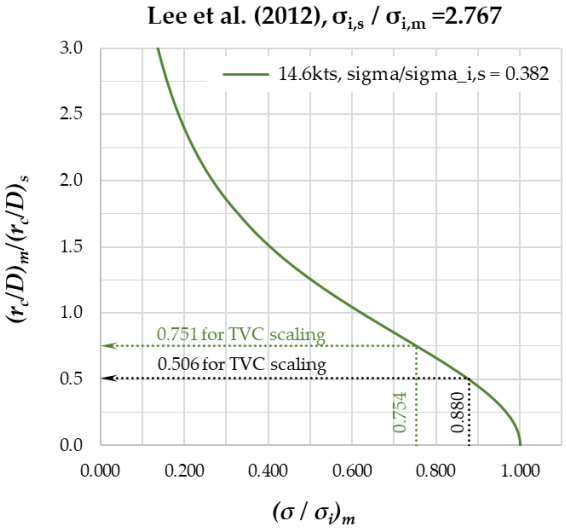

Figure 20. The ratio of the nondimensionalized tip vortex cavity radius according to the model cavitation number for the condition of V_s = 14.6kts

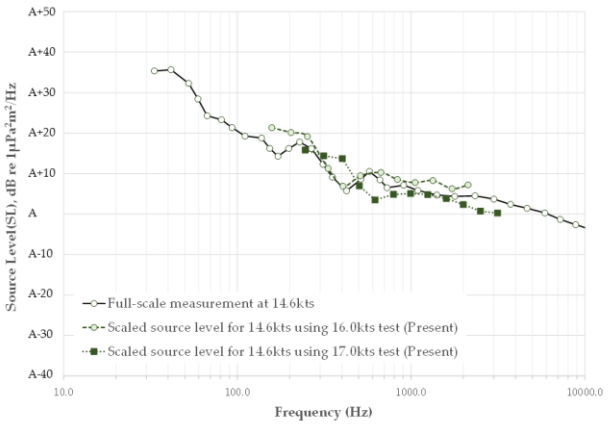

Figure 21. Comparison between the full-scale measurement result at 14.6kts by Lee et. al (2012) and the scaled source level using the model test result with the equivalent cavitation numbers at 16.0kts and 17.0kts

The smaller noise level scaling from the larger model scale noise level measured with a larger tip vortex cavity at 17.0kts condition makes a similar scaled source level to the predicted one using the model test results at 16.0kts. The noise level predictions from the model test at 16.0kts and 17.0kts are compared with the full-scale measurement at the target ship speed in Figure 21.

One model test case to scale the noise sources of different ship speed conditions is used in the second approach. The target ship speed conditions are 11.8kts and 14.6kts. The noise measurement of the model propeller at the condition of 16.0kts is used in the scaling procedure. Two curves describing the ratios of the nondimensionalized tip vortex cavity radius are provided in Figure 22.

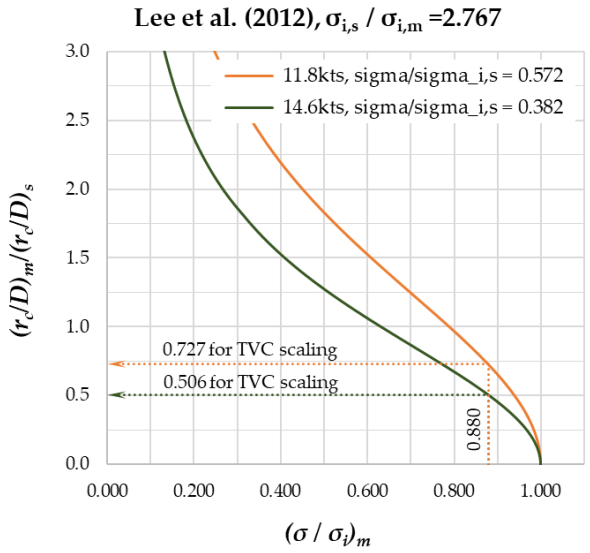

Figure 22. Scaling of tip vortex cavity size for 11.8kts and 14.6kts with the model test result at $\sigma_{n,m}$ same as the full-scale cavitation number at 16.0kts of Lee et al. (2012)

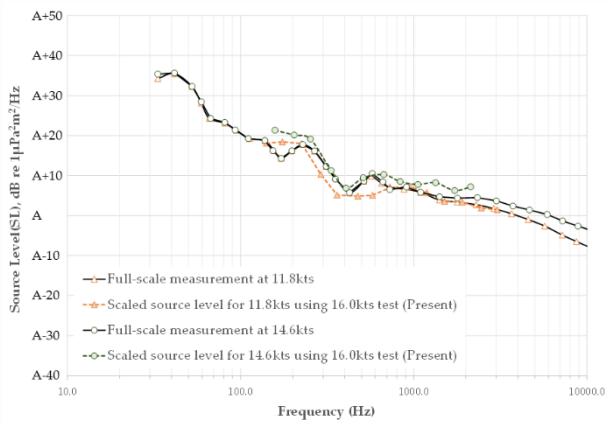

Figure 23. Comparison between the full-scale measurement results at 11.8kts and 14.6kts by Lee et al. (2012) and the scaled source level using the model test result at $\sigma_{n,m}$ same as the full-scale cavitation number at 16.0kts

The reproduced tip vortex cavity size at 0.880 of $(\sigma/\sigma_i)_m$ is 72.7% of the nondimensionalized cavity radius at 11.8kts of ship speed, and 50.6% of that at 14.6kts. These ratios are used in the scaling procedure with Equation (18) and the resultant scaled source levels are compared with each full-scale measurement result as shown in Figure 23. The scaled source levels are properly estimated from the same noise source level measured at the cavitation number at 16.0kts. This case study suggests that the noise measurement of the model propeller at only one test condition can be scaled into various full-scale ship speed conditions with an isolated tip vortex cavitation.

The noise scaling result of the target vessel introduced in Section 3 is finally evaluated and compared with the full-scale measurement result as shown in Figure 24. The noise measurement result of the model propeller at the same cavitation number at 11.1kts is used, and $(r_c/D)_m/(r_c/D)_s$ is 0.568 as presented in Figure 7. The range of error based on the sensitivity study in Chapter 3 is also added in this comparison. The scaled source level generally agrees well with the full-scale measurement data.

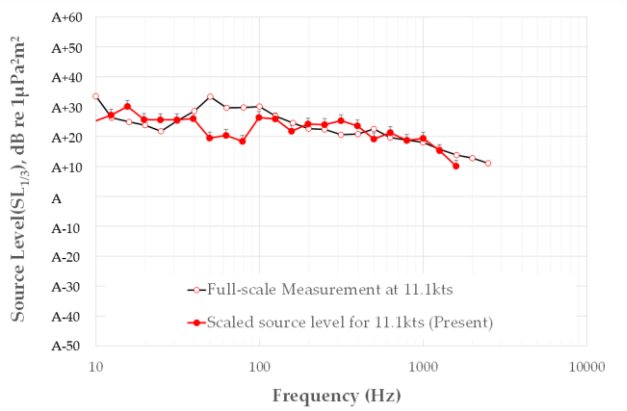

Figure 24. Comparison between the full-scale measurement results and the scaled source level using the model test result at the same cavitation number at 11.1kts

5 CONCLUSION

The noise scaling method was proposed to consider the viscous effect of the tip vortex cavitation. The relative size of the tip vortex cavity decreases in the model test at the same cavitation number of the full-scale condition due to the viscous scale effect. The scaling relation considering this relative size of the tip vortex cavitation has been derived based on the previous works on the acoustic scaling relation from the bubble dynamics. The relative size of the tip vortex cavity is necessary for the proposed noise level scaling. The relation between the cavity radius and the cavitation number has been derived using Proctor's empirical vortex model. The effect of the errors in the major components of the empirical vortex model on the scaled source level was investigated. There was a

reasonable allowance for each error of the component in the application of the present tip vortex scaling method.

The equivalent cavitation number of the model test to reproduce the same nondimensionalized tip vortex cavity radius as that of the full-scale propeller can be achieved. It was found that the scaling exponent on the ratio of Reynolds number for the equivalent developed tip vortex cavitation decreases along the cavitation number from the value at inception condition. The additional tip vortex cavity scaling is not necessary if the model test with an isolated tip vortex cavitation is possible at the equivalent cavitation number. The other case is more typical. A different type of cavitation, most often sheet cavitation, occurs together with the tip vortex cavitation at the equivalent cavitation number in many propeller designs. Additional tip vortex scaling after the noise measurement of the model propeller at the cavitation number as near as possible to the equivalent cavitation number is an alternative method of noise scaling in this case.

The present tip vortex cavitation scaling method has been applied to three validation cases and acceptable agreements were achieved. The noise measurement of the model propeller at one cavitation number with an isolated tip vortex cavitation can be used to predict scaled noise source level at any operating point having a tip vortex cavity only.

The proposed method is focused on the isolated tip vortex cavitation. There is a limitation that the present method cannot be applied to the scaling noise from the mixed type of cavitation. However, the scaling method for the isolated tip vortex cavitation could apply to various practical cases of merchant ships because the isolated tip vortex cavitation is a typical pattern at the quiet cruise condition of the merchant ships. The proposed tip vortex scaling method is able to be used not only in the scaling procedure but also in the decision of the proper test condition during the model test preparation.

REFERENCES

Aktas, B., Atlar, M., Turkmen, S., Shi, W., Sampson, R., Korkut, E. & Fitzsimmons, P. (2016). 'Propeller cavitation noise investigations of a research vessel using medium-size cavitation tunnel tests and full-scale trials'. Ocean Engineering. **120(2016), 122–135**.

American Bureau of Shipping (ABS) (2020). GUIDE FOR THE CLASSIFICATION NOTATION. 'Underwater noise and external airborne noise'.

Baiter, H.-J. (1985). 'On the Theoretical Background of Cavitation Noise Scaling'. Technical Report IHAK-TN 218/85, Fraunhofer Institute for Hydroacoustics, Ottobrunn, Germany.

Bosschers, J. (2018). 'Propeller tip-vortex cavitation and its broadband noise'. PhD thesis University of Twente, Netherlands.

Bosschers, J. (2020). 'The Effect of Reynolds Number on a Developed Tip-Vortex Cavity and its Radiated Noise'. 33rd Symposium on Naval Hydrodynamics, Osaka, Japan

Det Norske Veritas (DNV) (2015). Rules for classification: Ships, Part 6 Additional class notations, Chapter 7 Environmental protection and pollution control

Hommes, T., Bosschers, J. & Hoeijmakers, H. W. M. (2015). 'Evaluation of the radial pressure distribution of vortex models and comparison with experimental data'. Journal of Physics: **Conference Series 656 (2015) 012182**

ITTC (2021). Model Scale Noise Measurements, Recommended Procedures and Guidelines. 7.5-02-03-03.9

Korean Register (KR) (2022). Guidance for underwater radiated noise

Lee, J., Jung, J., Lee,K., Han, J., Park,H. & Seo, J. (2012). 'EXPERIMENTAL ESTIMATION OF A SCALING EXPONENT FOR TIP VORTEX CAVITATION VIA ITS INCEPTION TEST IN FULL-AND MODEL-SHIP'. Journal of Hydrodynamics, **24(5):658-667**

Levkovskii, V. L. (1968). 'Modeling of Cavitation Noise'. Soviet Physics Acoustics, **13(1), pp. 337-339**.

Lloyd's Register (LR) (2018). ShipRight, Design and Construction, Additional Design and Construction Procedure for the Determination of a Vessel's Underwater Radiated Noise

McCormick, B.W. (1962). 'On cavitation produced by a vortex trailing from a lifting surface'. Journal of Basic Engineering, **84(3), 369-379**

Oshima, A. (1990). 'A study on correlation of vortex cavitation noise of propeller measured in model experiments and full scale'. Journal of the Society of Naval Architects of Japan, **168(1):89–96**

Park, C., Kim, G., Yim, G., Park, Y. & Moon, I. (2019). 'The validation of model test for propeller cavitation noise prediction'. Proceedings of AMT'19, Rome, Italy

Park, C., Kim, G., Yim, G., Park, Y. & Moon, I. (2020). 'A validation study of the model test method for propeller cavitation noise prediction'. Ocean Engineering, **213 (2020), 107655**

Park, I., Kim, J., Paik, B. & Seol, H. (2021). 'Numerical study on tip vortex cavitation inception on a foil'. Applied Sciences, **2021, 11, 7332**

Park, J. & Seong, W. (2017). 'Novel scaling law for estimating propeller tip vortex cavitation noise from model experiment'. Journal of Hydrodynamics, **29(6), 962-971**

Proctor, F., Ahmad, N., Switzer, G. & Limon Duparcmeur, F. (2010). 'Three-phased wake vortex decay'. AIAA Atmospheric and Space Environments Conference, **2010-7991**, Toronto, Ontario, Canada

Ross, D. (1987). ‘Mechanics of Underwater Noise’. Peninsula Publishing.

Strasberg, M. (1977). ‘Propeller cavitation noise after 35 years of study’. In ASME Noise and Fluids Engineering.

Shen, Y. T., Gowing, S. & Jessup, S. (2009). ‘Tip vortex cavitation inception scaling for high Reynolds number applications’. Journal of Fluids Engineering. **Vol. 131, 071301-1**

Tani, G., Viviani, M., Felli, M., Lafeber, F. H., Lloyd, T., Aktas, B., Atlar, M., Turkmen, S., Seol, H., Hallander, J. & Sakamoto, N. (2020). ‘Noise measurements of a cavitating propeller in different facilities: Results of the round robin test programme’. Ocean Engineering. **213 (2020) 107599**